



## Preparation and evaluation of conjugate nanogels of glycylic-prednisolone with natural anionic polysaccharides as anti-arthritic delivery systems

Kohei Mizuno, Yuri Ikeuchi-Takahashi, Yoshiyuki Hattori & Hiraku Onishi

**To cite this article:** Kohei Mizuno, Yuri Ikeuchi-Takahashi, Yoshiyuki Hattori & Hiraku Onishi (2021) Preparation and evaluation of conjugate nanogels of glycylic-prednisolone with natural anionic polysaccharides as anti-arthritic delivery systems, *Drug Delivery*, 28:1, 136-144, DOI: [10.1080/10717544.2020.1865478](https://doi.org/10.1080/10717544.2020.1865478)

**To link to this article:** <https://doi.org/10.1080/10717544.2020.1865478>



© 2020 The Author(s). Published by Informa UK Limited, trading as Taylor & Francis Group.



Published online: 29 Dec 2020.



Submit your article to this journal [↗](#)



Article views: 2208



View related articles [↗](#)



View Crossmark data [↗](#)



Citing articles: 4 View citing articles [↗](#)

## Preparation and evaluation of conjugate nanogels of glycylic-prednisolone with natural anionic polysaccharides as anti-arthritic delivery systems

Kohei Mizuno, Yuri Ikeuchi-Takahashi, Yoshiyuki Hattori and Hiraku Onishi

Department of Drug Delivery Research, Hoshi University, Tokyo, Japan

### ABSTRACT

Although prednisolone (PD) is used as an anti-arthritis drug due to its rapid and strong anti-inflammatory potential, its frequent and large dosing often brings about adverse effects. Therefore, targeting therapy has attracted increasing attention to overcome such adverse effects. In the present study, nanogels (NGs) composed of macromolecule–PD conjugates were developed as a novel targeting delivery system, and their anti-inflammatory potential was examined. Conjugates were prepared by carbodiimide coupling between glycylic-prednisolone (GP) and the natural anionic polysaccharides, alginic acid (AL) and hyaluronic acid (HA). NGs were produced by the evaporation of organic solvent from the conjugate solution. The obtained NGs, named AL-GP-NG and HA-GP-NG, respectively, were examined for particle characteristics, *in vitro* release, pharmacokinetics, and *in vivo* efficacy. Both NGs were several hundred nanometers in size, had negative zeta potentials, and several % (w/w) drug contents. They released PD gradually at pH 7.4 and 6. They exhibited fairly good retention in the systemic circulation. In the efficacy examination using rats with adjuvant-induced arthritis, both NGs showed the stronger and more prolonged suppression of paw inflammation than PD alone. These suggested that the present NGs should be possibly useful as anti-arthritis targeting therapeutic systems.

### ARTICLE HISTORY

Received 13 October 2020  
Revised 11 December 2020  
Accepted 14 December 2020

### KEYWORDS

Conjugate nanogel; prednisolone; natural anionic polysaccharide; anti-arthritis; efficacy

## 1. Introduction

Rheumatoid arthritis (RA) is a chronic autoimmune disease (Calabresi et al., 2018). It affects 0.5–1% of the population worldwide, particularly developed countries (Bax et al., 2011; Cassone et al., 2020). RA is characterized by joint inflammation and the progressive destruction of cartilage, and affects diarthrodial joints (Choy, 2012). This immune disorder primarily develops at synovial tissue, leading to inflammation and invasion of the synovium as well as the destruction of cartilage and bone (Andreas et al., 2008). Regarding its etiology, genetic and environmental factors are essentially associated with the induction of RA (Cojocar & Chicoş, 2013; Glant et al., 2014).

In the treatment of RA, pharmacotherapy is very important. Commonly used medications include disease-modifying anti-rheumatic drugs, nonsteroidal anti-inflammatory drugs, glucocorticoids, and biologics (Boers et al., 1997; Ash & Emery, 2012; Yang et al., 2017; Abbasi et al., 2019). Although biologics such as antibody drugs, which are very effective, are becoming more widely used, they are associated with a risk of adverse effects and are expensive (Silva et al., 2010; Carter et al., 2012). Therefore, conventional drugs are still important and widely used in the treatment of RA.

Glucocorticoids are highly effective against RA (Walz et al., 1971). They suppress inflammation more rapidly and strongly than other types of drugs (Ward & Cloud, 1966).

Prednisolone (PD), an anti-inflammatory steroidal agent, is widely used in the treatment of RA (Buttgereit et al., 2008, 2013). As PD exhibits hormonal activities in various tissues in the body; adverse effects have to be managed in its use. Frequent dosing with moderate and/or high amounts of PD often causes adverse effects, such as diabetes, osteoporosis, glaucoma, and arteriosclerosis (Yano et al., 2002; Wang et al., 2007; Onishi et al., 2008; Kong et al., 2009; Van den Hoven et al., 2011). However, when the dose amount and/or dosing frequency are reduced, its efficacy decreases. Therefore, the specific delivery of PD to the diseased site is required in order to resolve these issues.

In the present study, nanogels (NGs), composed of macromolecular prodrugs of PD, were developed. In general, a NG is a kind of nanoparticle. NGs are three-dimensional nano-sized hydrogels formed by physical or chemical crosslinking of polymers (Boridy et al., 2009; Bae & Na, 2010; Kim et al., 2019). NGs are not dissolved in water, but hydrophilic parts swell. Thus, NGs have both characteristics of hydrogels and nanoparticles. In the conjugates composed of water-soluble polymer and hydrophobic small molecules, their self-assembly is brought about among the hydrophobic ligands, leading to the formation of NGs in water. As to the detailed preparation of NGs, the solvent diffusion (Bae & Na, 2010; Onishi et al., 2019) and sonication method (Park et al., 2004; Boridy et al., 2009) have been reported. We previously reported the conjugate of chondroitin sulfate (CS) and

glycyl-prednisolone (GP), named CS-GP, which formed the NG at the condition of PD content of more than 4% (w/w).

The targeting delivery toward RA is based on the following concept. Neovascular vessels, being highly permeable, grow well in inflammatory regions, allowing macromolecules and nanoparticles to leak into the diseased sites (Metselaar et al., 2003; Taylor & Sivakumar, 2005; Pandya et al., 2006). NGs, having nanoparticle characteristics, can be targeted to the inflammatory regions, which is similar to enhanced permeability and retention (EPR) effect in the tumor tissues (Matsumura & Maeda, 1986).

In the present study, we focused on alginic acid (AL) and hyaluronic acid (HA), which are actively examined in medical fields because of their highly biocompatible properties. AL is used as a biomaterial for wound dressings, etc. (Cabrera et al., 2005; Moscovici, 2015; Severino et al., 2019). HA is widely distributed in the connective tissues of the animal body, and is used as a therapeutic agent or material for drug carriers (Fraser et al., 1981; Hirakura et al., 2010; Kim et al., 2019). As these polymers are highly water-soluble, their conjugates with PD were considered to form the NGs due to the hydrophobicity of PD. As to previously reported CS-GP, the water-soluble type of CS-GP, injected intravenously, was eliminated fairly rapidly from the blood circulation, resulting in the fact that it did not exhibit so prolonged anti-inflammatory effects (Onishi et al., 2013, 2014); though the NG type of CS-GP was not tested. CS itself was reported to undergo a fairly rapid systemic clearance and degradation. Considering these features of CS and CS-GP, we here attempted to examine the potential of AL and HA as NG carriers for the targeting therapy against arthritis. Namely, the preparation of the conjugates of GP with AL and HA, and formation of their NGs, their *in vitro* properties and *in vivo* therapeutic profiles were demonstrated.

## 2. Materials and methods

### 2.1. Materials

Prednisolone, carbonyl-diimidazole (CDI), dimethyl-aminopyridine (DMAP), *N*-hydroxysuccinimide (NHS), 1-(3-dimethylaminopropyl)-3-ethylcarbodiimide hydrochloride (WSC), and sodium alginate (AL-Na; low viscosity grade (viscosity of 1% aqueous solution at 25 °C = 32.7 ± 0.4 mPa·s ( $n = 3$ )), cat no. 154725, lot no. QR13046) were purchased from FUJIFILM Wako Pure Chemical Corp. (Osaka, Japan). *N*-Tributyl-glycine (Tr-G) was obtained from Sigma-Aldrich Co., LLC. (St. Louis, MO). Hyaluronic acid (viscosity of 1% aqueous solution at 25 °C = 1.2 ± 0.1 mPa·s ( $n = 3$ )), product code H0595, lot no. 8FUKM-CI) was purchased from Tokyo Chemical Industry Co., Ltd. (Tokyo, Japan). Non-viable and desiccated *Mycobacterium tuberculosis* H37 Ra was obtained from Becton, Dickinson and Company (Franklin Lakes, NJ) and used in the preparation of adjuvants. All other chemicals were of reagent grade.

### 2.2. Animals

Female Lewis rats (160–170 g) were purchased from Charles River Laboratories Japan, Inc. (Yokohama, Japan). They were bred on the breeding diet MF (Oriental Yeast, Co., Ltd., Tokyo, Japan) with water *ad libitum*. Regarding the conditions of the animal room, temperature was set at 23 ± 1 °C, relative humidity was maintained at 60 ± 1%, and the light-dark cycle was 12 h. The experimental protocol was approved by the Committee on Animal Research of Hoshi University (Tokyo, Japan), in which the approval code was 30-076 (approval date: April 20 2018). Animal experiments were conducted based on the Guiding Principles for the Care and Use of Laboratory Animals of Hoshi University (Tokyo, Japan).

### 2.3. Preparation of conjugate nanogels

The conjugates of GP with AL and HA, named AL-GP and HA-GP, respectively, were synthesized as shown in Figure 1. The detailed procedure was as follows. First, the synthesis of Tr-G ester of PD (Tr-GP) was conducted according to the method described by Onishi & Matsuyama (2013). First, Tr-G (477 mg, 1.5 mmol) and CDI (243 mg, 1.5 mmol) were stirred in 10 mL tetrahydrofuran (THF) at 0 °C for 30 min, and DMAP (15 mg, 0.12 mmol) and PD (270 mg, 0.75 mmol) were then added and stirred at room temperature for 4.5 h. After evaporation of the solvent, Tr-GP was recrystallized using methanol. The chemical structure of Tr-GP was confirmed by the measurements of proton nuclear magnetic resonance (<sup>1</sup>H NMR) and electron ionization mass spectrometry (EI-MS). <sup>1</sup>H NMR (DMSO-d<sub>6</sub>),  $\delta$  (ppm): 7.20–7.42 (m, 16H, Tr-G Tr-H, PD C1-H), 6.15–6.18 (d, 1H, PD C2-H), 5.92 (s, 1H, PD C4-H), 5.02–5.05 (d, 1H, PD C21-H), 4.72–4.75 (d, 1H, PD C21-H'), 4.29 (s, 1H, PD C11-H), 2.97–2.99 (m, 2H, Tr-G C-H2). EI-MS  $m/z$ : 659 (M<sup>+</sup>).

Next, GP was obtained by detritylation of Tr-GP: soon after Tr-GP (300 mg) was dissolved in 75% (v/v) aqueous acetic acid (10 mL) by heating at 80 °C for 10 min, triphenylcarbinol was precipitated. Then, the mixture underwent ice cooling and filtration. The filtrate was evaporated with a rotary evaporator, and the residue was dissolved in the chloroform/methanol mixture. The resultant solution was chromatographed with a silica gel column using a chloroform/methanol mixture (15:1, v/v) as the elution solvent. The fractions of the major product (GP) were collected and evaporated to dryness. The structure of GP was confirmed by the measurements of <sup>1</sup>H NMR and matrix-assisted laser desorption/ionization-time of flight mass spectrometry (MALDI-TOF-MS). <sup>1</sup>H NMR (DMSO-d<sub>6</sub>),  $\delta$  (ppm): 7.31–7.33 (d, 1H, PD C1-H), 6.15–6.17 (d, 1H, PD C2-H), 5.92 (s, 1H, PD C4-H), 4.97–5.00 (d, 1H, PD C21-H), 4.84–4.87 (d, 1H, PD C21-H'), 4.27–4.38 (m, 3H, glycine C-H2, PD C11-H). MALDI-TOF-MS  $m/z$ : 418.54 ([M + H]<sup>+</sup>).

Finally, the conjugates of GP with the polysaccharides were prepared as follows. As to AL-GP, after GP (30 mg) and AL-Na (60 mg) were dissolved in 10 mL of the THF/water (1:1, v/v) mixture, WSC (500 mg), and NHS (300 mg) were added, and the mixture was stirred at room temperature overnight.

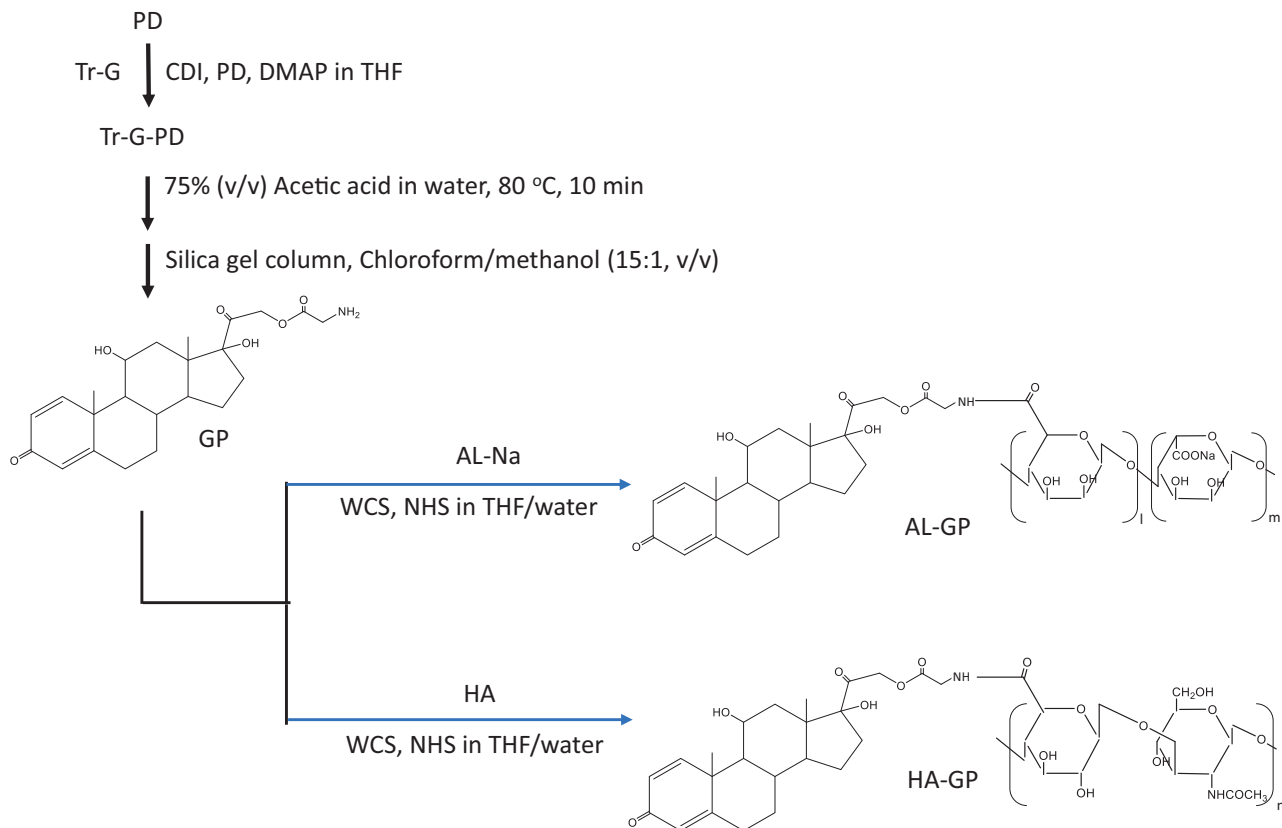


**Figure 1.** Synthesis of AL-GP and HA-GP.

The resultant mixture was chromatographed with a Sephadex G50 gel column (2.6 cm (inner diameter) × 19 cm (length)) using a mixture of 0.1 M NaCl aqueous solution and methanol (7:3, v/v) as the elution solvent. After the macromolecular fractions had been gathered, the solution obtained was dialyzed against water at 4 °C. The medium remaining in the dialysis bag was lyophilized to yield AL-GP powder. HA-GP was prepared in the same manner, except for the use of HA (60 mg) instead of AL-Na (60 mg).

The NGs of AL-GP and HA-GP, named AL-GP-NG and HA-GP-NG, respectively, were obtained by the solvent evaporation technique (Figure 2). After the conjugate was dissolved in the mixture of THF and water, THF was evaporated gradually using a rotary evaporator *in vacuo* until THF was removed completely from the solvent. The NG was obtained as a white suspension in water.

#### 2.4. Characterization of NGs

The drug contents of AL-GP-NG and HA-GP-NG were examined by the complete liberation of PD from NGs followed by spectrophotometric measurements. The NGs, AL-Na, and HA (3 mg) were placed in 5 mL of 0.1 M NaOH aqueous solution and incubated at 45 °C for 10 min. After the media were centrifuged, supernatants were measured spectrophotometrically at 246 nm. The difference in absorbance at 246 nm between that supernatant and polysaccharide solution was obtained as a net absorbance by the conjugated PD. The amount of the conjugated PD was calculated by comparing the net

absorbance (246 nm) with the absorbance of PD itself in 0.1 M NaOH aqueous solution (246 nm).

The particle size and zeta potential of each NG were analyzed using the dynamic light scattering apparatus, ELS-Z2 (Otsuka Electronics Co., Ltd., Osaka, Japan).

#### 2.5. In vitro drug release from NGs

AL-GP-NG and HA-GP-NG were suspended in phosphate-buffered saline of pH 7.4 (PBS) and 0.1 M acetate buffer of pH 6.0 at a concentration of 2 mg/mL. The suspension (4 mL) was placed in a cellulose dialysis tube (MW cutoff 14,000) made by Viskase Companies, Inc. (Darien, IL). The tube containing the NG sample was completely immersed in 16 mL of PBS or acetate buffer, and incubated at 37 °C by shaking horizontally at 60 rpm for 48 h. Aliquot samples (50 μL) were taken at appropriate time points. Immediately after sampling, 100 μL of 0.1 M acetate buffer (pH 4) was added to the sample to suppress further release, because the carboxy ester is very stable around pH 4. The resultant mixture was analyzed by HPLC to measure the concentration of released PD.

#### 2.6. Plasma concentration studies after intravenous (i.v.) injection of NGs

AL-GP-NG and HA-GP-NG were suspended in saline at 2.5 mg PD eq./mL. The NG suspension was injected intravenously via the jugular vein into normal rats at 2.5 mg PD eq./kg. Blood samples (each 300 μL) were taken immediately before and 0.5, 1, 3, and 7 h after administration. After each sampling,

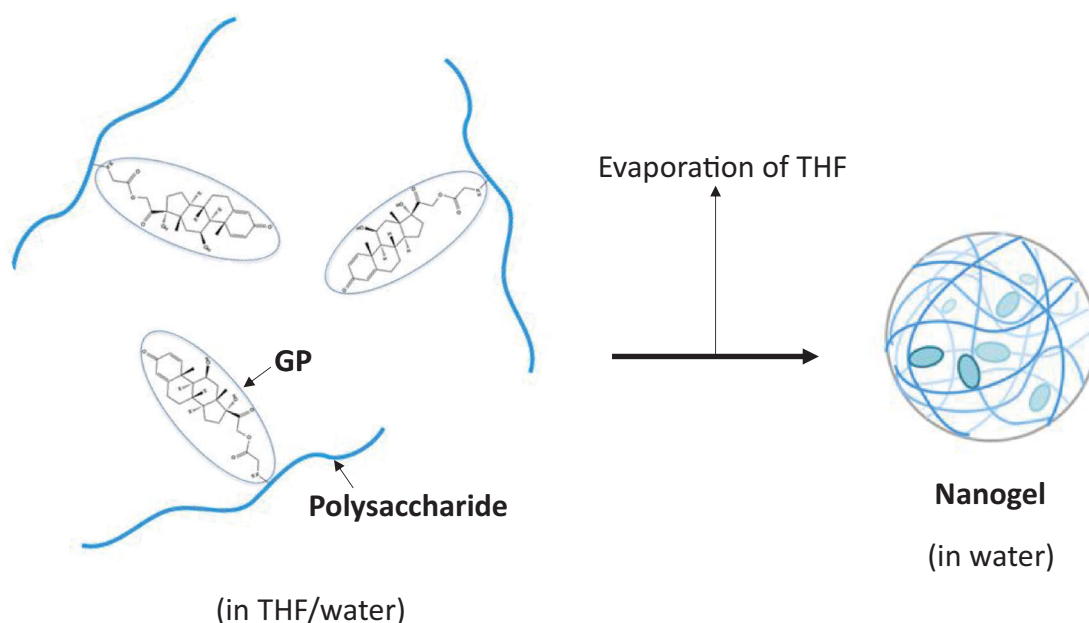


**Figure 2.** Schematic diagram of nanogel formation by organic solvent evaporation.

centrifugation was performed at 1500 rpm to obtain plasma. Plasma (50  $\mu\text{L}$ ), 20% trichloroacetic acid (10  $\mu\text{L}$ ), and methanol (35  $\mu\text{L}$ ) were mixed and shaken vigorously for 5 min. After centrifugation of the mixture, the supernatant was analyzed by HPLC to assess the concentration of free PD.

The concentration of total (free + conjugated) PD was analyzed as follows: plasma (50  $\mu\text{L}$ ) and 0.1 M NaOH aqueous solution (50  $\mu\text{L}$ ) were mixed, and the mixture was incubated at 45  $^{\circ}\text{C}$  for 10 min. Then, 0.1 M HCl aqueous solution (50  $\mu\text{L}$ ) was added to neutralize the sample pH. Furthermore, 20% trichloroacetic acid (30  $\mu\text{L}$ ) and methanol (105  $\mu\text{L}$ ) added, and the mixture underwent vigorous shaking for 5 min. After centrifugation of the sample, the supernatant was analyzed by HPLC to determine the concentration of PD.

As the control, PD alone, dissolved in 50% (w/v) polyethylene glycol 400 (PEG400) saline solution at 2.5 mg/mL, was administered intravenously to normal rats via the jugular vein at 2.5 mg/kg. Blood sampling and analyses of the plasma concentration of PD were performed as in the case of the free PD in the NG suspension.

Pharmacokinetic parameters were calculated using the program MULTI produced by Yamaoka et al. (1981).

### 2.7. In vivo examination of efficacy and adverse effects in rats with adjuvant-induced arthritis

*In vivo* experiments of efficacy and adverse effects were performed using rats with adjuvant-induced arthritis. The *in vivo* experimental schedules are shown in Figure 3. The arthritic animal models were produced according to the method described by Hirano et al. (1994) and Matsukuma et al. (2005). Non-viable and desiccated *M. tuberculosis* H37 Ra (20 mg) was suspended in 4 mL of liquid paraffin and ground in a mortar. The resultant suspension (100  $\mu\text{L}$ ) was injected intracutaneously into the foot pad of the right hind paw as

the adjuvant. Body weights and both hind paw volumes were measured every day after the injection of the adjuvant.

Drugs (NGs or PD alone) were administered intravenously at 2.5 mg PD eq./kg 15 and 16 d after the adjuvant injection; the drug administration was conducted in the manner of consecutive dosing at 2.5 mg PD eq./kg  $\times$  2 d. The control group received no treatment. Body weights and the volumes of both hind paws were monitored every day until 28 d after the adjuvant injection. Changes in body weight were examined as an index of adverse effects. The hind paw volume was investigated as an index of the degree of inflammation.

### 2.8. HPLC assay

A HPLC analysis was performed using an apparatus made by Shimadzu Corp. (Kyoto, Japan); A LC-20AD pump, SPD-20A UV/VIS detector, SIL-20AC autosampler, SLC-10A system controller, and LabSolutions system were used at room temperature. An YMC-Pack ODS-AM column (6 mm (inner diameter)  $\times$  150 mm (length)) was used as an analytical column. The detector was set at 246 nm.

In *in vitro* studies, a 30% (v/v) 2-propanol aqueous solution containing trifluoroacetic acid at 0.1% (w/v) was used as the mobile phase, and flowed at 1 mL/min. The sample (20  $\mu\text{L}$ ) was injected onto the column.

As to the analysis of samples in *in vivo* experiments, a mixture of acetonitrile and 50 mM sodium citrate-phosphoric acid buffer of pH 4.1 (35:65, v/v) was used as the mobile phase, and its flow rate was set at 1 mL/min. Each sample (20  $\mu\text{L}$ ) was injected on the column. The concentration of PD was calculated by the absolute calibration method.

### 2.9. Statistical analysis

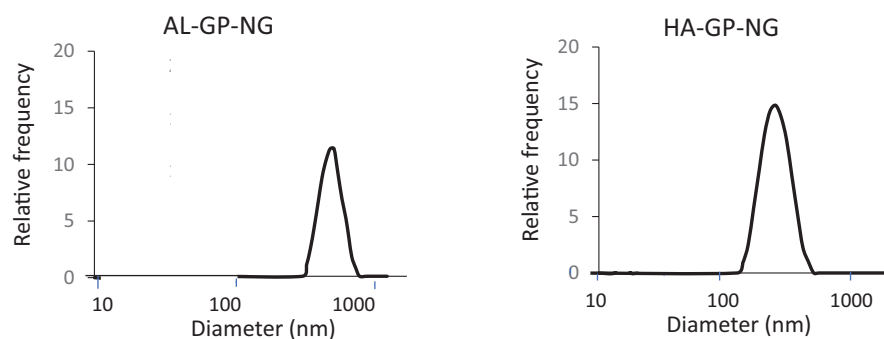
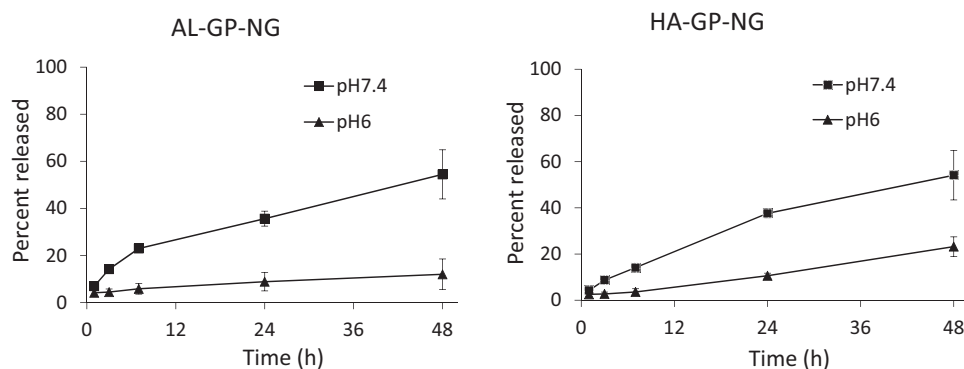
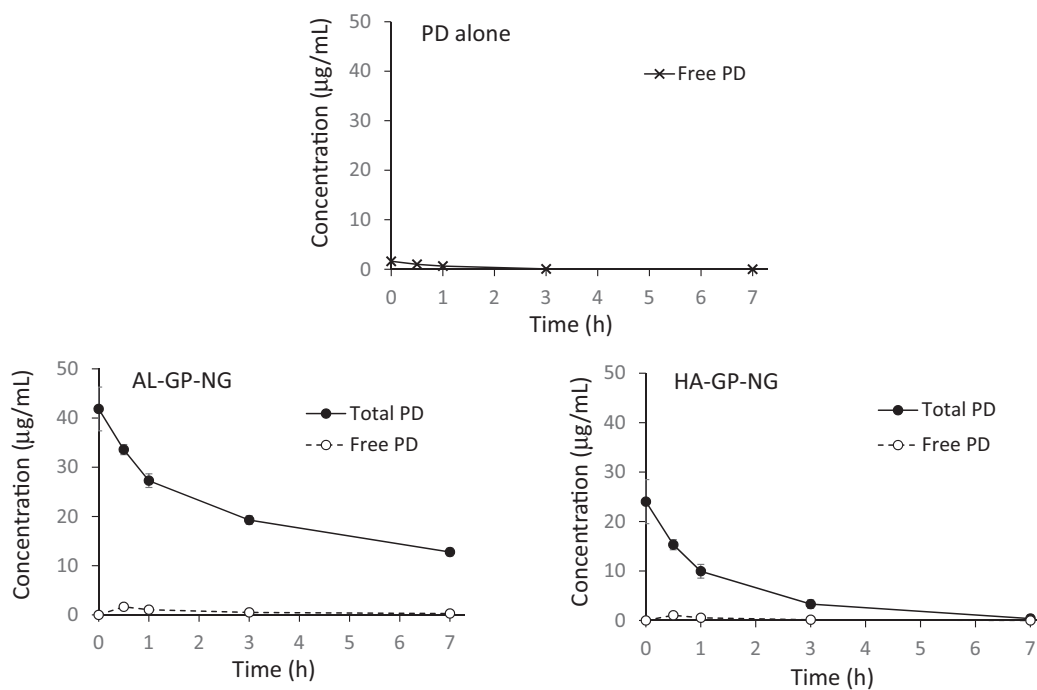
Statistical analyses were performed with a one-way ANOVA followed by Tukey's post hoc test, and the significance of differences was set as  $p < .05$ .



**Table 1.** Preparation of conjugate nanogels and their particle features.

Nanogel	AL-Na (mg)	HA (mg)	GP (mg)	WSC (mg)	NHS (mg)	PD content (% w/w)	Particle size <sup>a</sup> (nm)	Zeta potential <sup>a</sup> (mV)
AL-GP-NG	60	–	30	500	300	3.4	444 ± 88	–24.9 ± 0.6
HA-GP-NG	–	60	30	500	300	5.6	304 ± 63	–19.3 ± 0.6

<sup>a</sup>The results are expressed as the mean ± S.D. ( $n = 3$ ).


**Figure 4.** Size distributions of conjugate nanogels.

**Figure 5.** *In vitro* release of PD from conjugate nanogels at pH 6 and 7.4 at 37 °C. The results are expressed as the mean ± S.D. ( $n = 3$ ).

**Figure 6.** Plasma concentration–time profiles of free and total (free + conjugated) PD after i.v. administration of conjugate nanoparticles in normal rat. The results are expressed as the mean ± S.E. ( $n = 3$ ).

**Table 2.** Pharmacokinetic parameters of free and total PD in i.v. administration of AL-GP-NG to rats.

Preparation	Species	$C_{max}$ ( $\mu\text{g/mL}$ )	$T_{max}$ (h)	AUC (0–7 h) ( $\mu\text{g}\cdot\text{h/mL}$ )	MRT(0–7 h) (h)	VRT (0–7 h) ( $\text{h}^2$ )
PD alone	Free PD	$1.61 \pm 0.30$	$0.0 \pm 0.0$	$1.91 \pm 0.08$	$0.87 \pm 0.05$	$0.67 \pm 0.08$
AL-GP-NG	Free PD	$1.64 \pm 0.03$	$0.5 \pm 0.0$	$4.16 \pm 0.01$	$2.41 \pm 0.03^{**}$	$4.22 \pm 0.18^{**}$
	Total PD	$41.84 \pm 4.45^{**,\#\#}$	$0.0 \pm 0.0$	$144.69 \pm 4.97^{**,\#\#}$	$2.72 \pm 0.04^{**,\#\#}$	$5.06 \pm 0.06^{**,\#\#}$

The results are expressed as the mean  $\pm$  S.E. ( $n = 3$ ).

\*\* $p < .01$  vs. free PD (PD alone).

## $p < .01$  vs. free PD (AL-GP-NG).

**Table 3.** Pharmacokinetic parameters of free and total PD in i.v. administration of HA-GP-NG to rats.

Preparation	Species	$C_{max}$ ( $\mu\text{g/mL}$ )	$T_{max}$ (h)	AUC (0–7 h) ( $\mu\text{g}\cdot\text{h/mL}$ )	MRT (0–7 h) (h)	VRT (0–7 h) ( $\text{h}^2$ )
PD alone	Free PD	$1.61 \pm 0.30$	$0.0 \pm 0.0$	$1.91 \pm 0.08$	$0.87 \pm 0.05$	$0.67 \pm 0.08$
HA-GP-NG	Free PD	$1.05 \pm 0.10$	$0.5 \pm 0.0$	$1.61 \pm 0.18$	$1.37 \pm 0.16^*$	$0.97 \pm 0.18$
	Total PD	$24.03 \pm 3.08^{**,\#\#}$	$0.0 \pm 0.0$	$36.77 \pm 3.91^{**,\#\#}$	$1.38 \pm 0.08^*$	$1.86 \pm 0.08^{**,\#\#}$

The results are expressed as the mean  $\pm$  S.E. ( $n = 3$ ).

\* $p < .05$  vs. free PD (PD alone).

\*\* $p < .01$  vs. free PD (PD alone).

## $p < .01$  vs. free PD (HA-GP-NG).

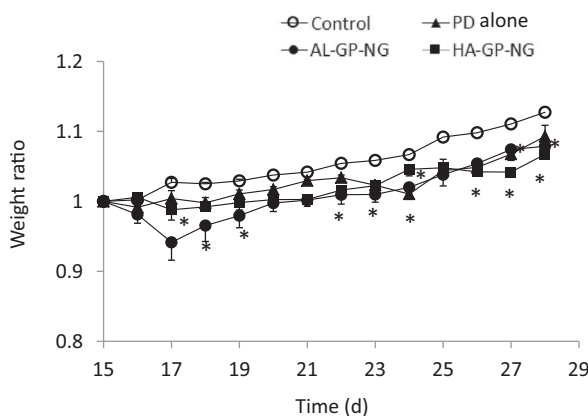


**Figure 7.** Change in body weight after i.v. administration of conjugate nanoparticles in rats with adjuvant-induced arthritis. The results are expressed as the mean  $\pm$  S.E. ( $n = 3$ ). \* $p < .05$  vs. control.

using the values at 0.5 and 1 h. Regarding the i.v. injection of PD alone, the plasma levels detected were very small. The mean plasma level was calculated to be less than  $2 \mu\text{g/mL}$  immediately after the i.v. administration.

Regarding the i.v. injection of AL-GP-NG, the total PD concentration was markedly higher than the free PD concentration. The total PD concentration was higher than  $40 \mu\text{g/mL}$  immediately after its administration, and was still higher than  $10 \mu\text{g/mL}$  at 7 h. The free PD concentration was maximal at 0.5 h, being  $1.64 \mu\text{g/mL}$ , and then the free PD concentration gradually decreased.

As to the i.v. injection of HA-GP-NG, total PD concentrations were also higher than free PD concentrations. The total PD level at 0 h was calculated at  $24.03 \mu\text{g/mL}$ . Overall, total PD levels were lower with HA-GP-NG than with AL-GP-NG. At 7 h, the total PD concentration decreased to  $0.39 \mu\text{g/mL}$ . The concentration of free PD was maximal at 0.5 h, being  $1.05 \mu\text{g/mL}$ , and was not detected at 7 h. The levels of free PD were also lower with HA-GP-NG than with AL-GP-NG.

The pharmacokinetic parameters of AL-GP-NG and HA-GP-NG are shown in Tables 2 and 3, respectively. Free PD by PD alone, free PD by NG, and total PD by NG were compared. In AL-GP-NG, total PD gave markedly higher  $C_{max}$ , AUC (0–7 h), MRT (0–7 h), and VRT (0–7 h) than free PD by PD alone and

NG. Higher MRT (0–7 h) and VRT (0–7 h) were observed in free PD with AL-GP-NG than in free PD by PD alone. HA-GP-NG also showed similar pharmacokinetic features to those of AL-GP-NG. Since both NGs gave higher total plasma concentrations and more prolonged systemic retention, suggesting that the NGs should work well as a targeting delivery system to the sites of inflammation.

### 3.4. Efficacy of NGs in rats with adjuvant-induced arthritis

Efficacy studies were performed using diseased model rats with adjuvant-induced arthritis. Changes in body weight after i.v. administration were examined as adverse effects. The anti-inflammatory effectiveness of each drug was evaluated from changes in hind paw volumes (Metselaar et al., 2003; Quan et al., 2010; Aono & Sasano, 2018). The body weight ratio and hind paw volume ratio were calculated using the following equations:

$$\begin{aligned} \text{Body weight ratio on day X} \\ = (\text{body weight on day X}) / (\text{body weight on day 15}) \end{aligned} \quad (1)$$

$$\begin{aligned} \text{Hind paw volume ratio on day X} \\ = (\text{hind paw volume on day X}) \\ / (\text{hind paw volume on day 15}) \end{aligned} \quad (2)$$

The body weight change, obtained by Equation (1), is shown in Figure 7. Although PD alone and NGs induced a small decrease in body weight in the early periods, this reduction quickly recovered. The anti-inflammatory effects were evaluated from the hind paw volume ratios (Equation (2)). The results obtained are shown in Figure 8. Although PD alone only slightly decreased the paw volume, its anti-inflammatory effects were not strong and did not significantly differ from those of the control group. On the other hand, both NGs strongly suppressed the volumes of both hind paws. In both NGs, stronger suppressive effects were observed in the right hind paw for long periods. Also, both NGs suppressed the left hind paw volume better than PD alone. The suppressive effects were not so different between AL-GP-NG and

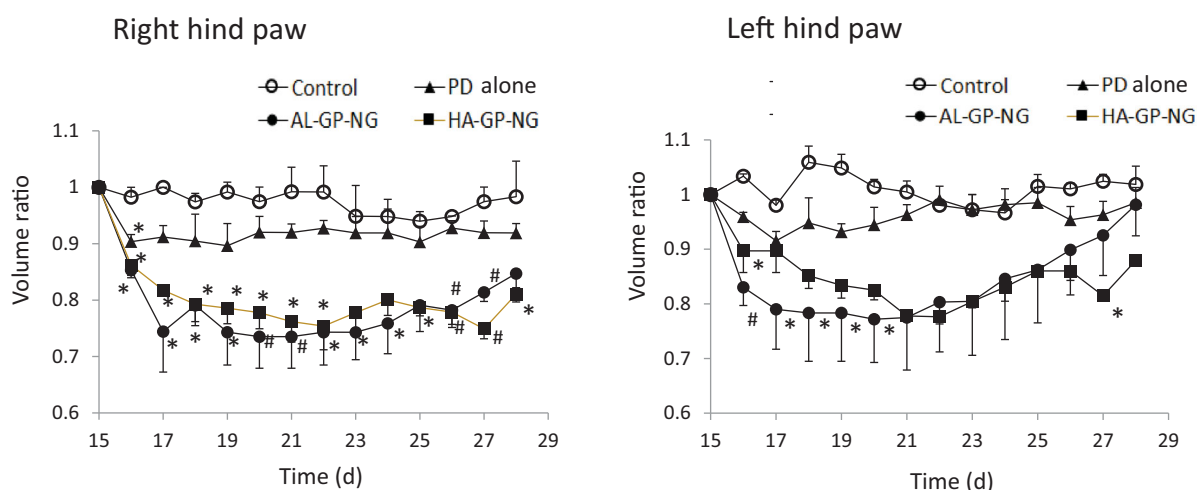


**Figure 8.** Change in body weight after i.v. administration of conjugate nanoparticles in rats with adjuvant-induced arthritis. The results are expressed as the mean  $\pm$  S.E. ( $n = 3$ ). \* $p < .05$  vs. control and # $p < .05$  vs. PD alone.

HA-GP-NG. As far as the profiles of the hind paw volume ratios were concerned, the present NGs appeared to show longer suppression of inflammation than the previously reported CS-SP conjugate (Onishi et al., 2013). The high efficacy of NGs against arthritis was considered to be due to their targeting ability to diseased sites. Targeting potential to arthritic sites will be elucidated in future studies.

#### 4. Conclusions

In the present study, the natural anionic polysaccharides, AL and HA, were derivatized by carbodiimide coupling with GP. The conjugates obtained formed NGs in water and were named AL-GP-NG and HA-GP-NG, respectively. Both NGs were several hundred nanometers in size, had negative zeta potentials, and several % (w/w) drug contents. They gradually released PD at approximately 30-40% per day at pH 7.4 and more slowly at pH 6. Furthermore, both NGs exhibited fairly good retention in the systemic circulation. These *in vitro* and *in vivo* features suggested that both NGs should have good targeting potential to arthritic sites through the high permeability of the neovascular vessels of the inflammatory sites. In the efficacy studies using rats with adjuvant-induced arthritis, both the present NGs showed the strong and prolonged suppression of hind paw inflammation. Therefore, it was demonstrated that these NGs should be possibly useful in the treatment of arthritis.

#### Disclosure statement

No potential conflict of interest was reported by the author(s).

#### References

Abbasi M, Mousavi MJ, Jamalzei S, et al. (2019). Strategies toward rheumatoid arthritis therapy; the old and the new. *J Cell Physiol* 234: 10018-31.

- Andreas K, Lübke C, Häupl T, et al. (2008). Key regulatory molecules of cartilage destruction in rheumatoid arthritis: an *in vitro* study. *Arthritis Res Ther* 10:R9.
- Aono H, Sasano M. (2018). Animal models for rheumatoid arthritis. *Clin Rheumatol Relat Res* 30:28-37.
- Ash Z, Emery P. (2012). The role of tocilizumab in the management of rheumatoid arthritis. *Expert Opin Biol Ther* 12:1277-89.
- Bae BC, Na K. (2010). Self-quenching polysaccharide-based nanogels of pullulan/folate-photosensitizer conjugates for photodynamic therapy. *Biomaterials* 31:6325-635.
- Bax M, van Heemst J, Huizinga TW, et al. (2011). Genetics of rheumatoid arthritis: what have we learned? *Immunogenetics* 63:459-66.
- Boers M, Verhoeven AC, Markusse HM, et al. (1997). Randomised comparison of combined step-down prednisolone, methotrexate and sulphasalazine with sulphasalazine alone in early rheumatoid arthritis. *Lancet* 350:309-18.
- Boridy S, Takahashi H, Akiyoshi K, Maysinger D. (2009). The binding of pullulan modified cholesteryl nanogels to Abeta oligomers and their suppression of cytotoxicity. *Biomaterials* 30:5583-91.
- Buttgereit F, Doering G, Schaeffler A, et al. (2008). Efficacy of modified-release versus standard prednisone to reduce duration of morning stiffness of the joints in rheumatoid arthritis (CAPRA-1): a double-blind, randomised controlled trial. *Lancet* 371:205-14.
- Buttgereit F, Mehta D, Kirwan J, et al. (2013). Low-dose prednisone chronotherapy for rheumatoid arthritis: a randomised clinical trial (CAPRA-2). *Ann Rheum Dis* 72:204-10.
- Cabrales P, Tsai AG, Intaglietta M. (2005). Alginate plasma expander maintains perfusion and plasma viscosity during extreme hemodilution. *Am J Physiol Heart Circ Physiol* 288:H1708-H16.
- Calabresi E, Petrelli F, Bonifacio AF, et al. (2018). One year in review 2018: pathogenesis of rheumatoid arthritis. *Clin Exp Rheumatol* 36: 175-84.
- Carter CT, Changolkar AK, McKenzie RS. (2012). Adalimumab, etanercept, and infliximab utilization patterns and drug costs among rheumatoid arthritis patients. *J Med Econ* 15:332-9.
- Cassone G, Manfredi A, Vacchi C, et al. (2020). Treatment of rheumatoid arthritis-associated interstitial lung disease: lights and shadows. *J Clin Med* 9:1082.
- Choy E. (2012). Understanding the dynamics: pathways involved in the pathogenesis of rheumatoid arthritis. *Rheumatology* 51:v3-v11.
- Cojocaru M, Chicoş B. (2013). Genetic differences between patients with rheumatoid arthritis. *Rom J Intern Med* 51:89-91.
- Fraser JR, Laurent TC, Pertoft H, et al. (1981). Plasma clearance, tissue distribution and metabolism of hyaluronic acid injected intravenously in the rabbit. *Biochem J* 200:415-24.
- Glant TT, Mikecz K, Rauch TA. (2014). Epigenetics in the pathogenesis of rheumatoid arthritis. *BMC Med* 12:35.

- Goldie I, Nachemson A. (1969). Synovial pH in rheumatoid knee-joints. I. The effect of synovectomy. *Acta Orthop Scand* 40:634–41.
- Hirakura T, Yasugi K, Nemoto T, et al. (2010). Hybrid hyaluronan hydrogel encapsulating nanogel as a protein nanocarrier: new system for sustained delivery of protein with a chaperone-like function. *J Control Release* 142:483–9.
- Hirano S, Wakazono K, Agata N, et al. (1994). Effects of cytogenin, a novel anti-arthritis agent, on type II collagen-induced arthritis in DBA/1J mice and adjuvant arthritis in Lewis rats. *Int J Tissue React* 16: 155–62.
- Kim K, Choi H, Choi ES, et al. (2019). Hyaluronic acid-coated nanomedicine for targeted cancer therapy. *Pharmaceutics* 11:301.
- Kong H, Lee Y, Hong S, et al. (2009). Sulfate-conjugated methylprednisolone as a colon-targeted methylprednisolone prodrug with improved therapeutic properties against rat colitis. *J Drug Target* 17:450–8.
- Matsukuma H, Nakanishi H, Kawahara S, et al. (2005). Anti-inflammatory effect of moxibustion on adjuvant-induced arthritis. *J Jpn Soc Balneol Climatol Phys Med* 68:181–8.
- Matsumura Y, Maeda H. (1986). A new concept for macromolecular therapeutics in cancer chemotherapy: mechanism of tumorotropic accumulation of proteins and the antitumor agent smancs. *Cancer Res* 46:6387–92.
- Metselaar JM, Wauben MH, Wagenaar-Hilbers JP, et al. (2003). Complete remission of experimental arthritis by joint targeting of glucocorticoids with long-circulating liposomes. *Arthritis Rheum* 48:2059–66.
- Moscovici M. (2015). Present and future medical applications of microbial exopolysaccharides. *Front Microbiol* 6:1012.
- Onishi H, Ikeuchi-Takahashi Y, Kawano K, et al. (2019). Preparation of chondroitin sulfate–glycyl–prednisolone conjugate nanogel and its efficacy in rats with ulcerative colitis. *Biol Pharm Bull* 42:1155–63.
- Onishi H, Isoda Y, Matsuyama M. (2013). In vivo evaluation of chondroitin sulfate–glycyl–prednisolone for anti-arthritis effectiveness and pharmacokinetic characteristics. *Int J Pharm* 456:113–20.
- Onishi H, Matsuyama M. (2013). Conjugate between chondroitin sulfate and prednisolone with a glycine linker: preparation and in vitro conversion analysis. *Chem Pharm Bull (Tokyo)* 61:902–12.
- Onishi H, Oosegi T, Machida Y. (2008). Efficacy and toxicity of Eudragit-coated chitosan–succinyl–prednisolone conjugate microspheres using rats with 2,4,6-trinitrobenzenesulfonic acid-induced colitis. *Int J Pharm* 358:296–302.
- Onishi H, Yoshida R, Matsuyama M. (2014). Chondroitin sulfate–glycyl–prednisolone conjugate as arthritis targeting system: localization and drug release in inflammatory joints. *Biol Pharm Bull* 37:1641–9.
- Pandya NM, Dhalla NS, Santani DD. (2006). Angiogenesis—a new target for future therapy. *Vascul Pharmacol* 44:265–74.
- Park K, Kim K, Kwon IC, et al. (2004). Preparation and characterization of self-assembled nanoparticles of heparin–deoxycholic acid conjugates. *Langmuir* 20:11726–31.
- Quan LD, Yuan F, Liu XM, et al. (2010). Pharmacokinetic and biodistribution studies of N-(2-hydroxypropyl)methacrylamide copolymer–dexamethasone conjugates in adjuvant-induced arthritis rat model. *Mol Pharm* 7:1041–9.
- Ren H, He Y, Liang J, et al. (2019). Role of liposome size, surface charge, and PEGylation on rheumatoid arthritis targeting therapy. *ACS Appl Mater Interfaces* 11:20304–15.
- Severino P, da Silva CF, Andrade LN, et al. (2019). Alginate nanoparticles for drug delivery and targeting. *Curr Pharm Des* 25:1312–34.
- Silva LC, Ortigosa LC, Benard G. (2010). Anti-TNF- $\alpha$  agents in the treatment of immune-mediated inflammatory diseases: mechanisms of action and pitfalls. *Immunotherapy* 2:817–33.
- Taylor PC, Sivakumar B. (2005). Hypoxia and angiogenesis in rheumatoid arthritis. *Curr Opin Rheumatol* 17:293–8.
- van den Hoven JM, Hofkens W, Wauben MH, et al. (2011). Optimizing the therapeutic index of liposomal glucocorticoids in experimental arthritis. *Int J Pharm* 416:471–7.
- Walz DT, DiMartino MJ, Misher A. (1971). Adjuvant-induced arthritis in rats. II. Drug effects on physiologic, biochemical and immunologic parameters. *J Pharmacol Exp Ther* 178:223–31.
- Wang D, Miller SC, Liu XM, et al. (2007). Novel dexamethasone–HPMA copolymer conjugate and its potential application in treatment of rheumatoid arthritis. *Arthritis Res Ther* 9:R2.
- Ward JR, Cloud RS. (1966). Comparative effect of antirheumatic drugs on adjuvant-induced polyarthritis in rats. *J Pharmacol Exp Ther* 152: 116–21.
- Yamaoka K, Tanigawara Y, Nakagawa T, et al. (1981). A pharmacokinetic analysis program (multi) for microcomputer. *J Pharmacobiodyn* 4: 879–85.
- Yang M, Feng X, Ding J, et al. (2017). Nanotherapeutics relieve rheumatoid arthritis. *J Control Release* 252:108–24.
- Yano H, Hirayama F, Kamada M, et al. (2002). Colon-specific delivery of prednisolone-appended alpha-cyclodextrin conjugate: alleviation of systemic side effect after oral administration. *J Control Release* 79: 103–12.